Moiré phonons and impact of electronic symmetry breaking in twisted trilayer graphene

Rhine Samajdar [1], Yanting Teng,[1] and Mathias S. Scheurer [2]

[1]*Department of Physics, Harvard University, Cambridge, Massachusetts 02138, USA*
[2]*Institut für Theoretische Physik, Universität Innsbruck, A-6020 Innsbruck, Austria*

Twisted trilayer graphene is a particularly promising moiré superlattice system, due to its tunability, strong superconductivity, and complex electronic symmetry breaking. Motivated by these properties, we study lattice relaxation and the long-wavelength phonon modes of this system. We show that mirror-symmetric trilayer graphene hosts, aside from the conventional acoustic phonon modes, two classes of shear modes, which are even and odd under mirror reflection. The mirror-even modes are found to be gapless and equivalent to the "phason" modes of twisted bilayer graphene, with appropriately rescaled parameters. The modes odd under mirror symmetry have no analog in twisted bilayer graphene and exhibit a finite gap which we show is directly proportional to the degree of lattice relaxation. We also discuss the impact of mirror-symmetry breaking, which can be tuned by a displacement field or result from a stacking shift, and of rotational- as well as time-reversal-symmetry breaking, resulting from spontaneous electronic order. We demonstrate that this can induce finite angular momentum to the phonon branches. Our findings are important to the interpretation of recent experiments concerning the origin of superconductivity and of linear-in-T resistivity.

Introduction. Stacking and twisting different layers of graphene has emerged as a popular route to creating correlated superlattices over the last few years [1–5]. Besides the most well-studied system, twisted bilayer graphene (TBG), many other geometries have been explored both experimentally and theoretically. Among them, mirror-symmetric twisted trilayer graphene (TTG) [6–21], which consists of three graphene layers with alternating twist angles (see Fig. 1), stands out: it is the first system that can be efficiently tuned with a perpendicular displacement field D_0 while exhibiting strong and reproducible superconductivity. Recently, another unique behavior was observed experimentally on decreasing the twist angle θ slightly below the magic angle [12,13]: while the system still exhibits superconductivity with roughly the same critical temperature, the linear-in-temperature (T) resistivity seen at the magic angle disappears. Motivated by these outstanding properties of TTG and the fact that both superconductivity and linear-in-T resistivity [22,23] are considered to be linked to phonons in graphene moiré systems [23–29], here we theoretically study the long-wavelength and low-energy phonons of this system that are crucially determined by the moiré superlattice and thus depend on the twist angle.

Long-wavelength phonon modes have recently attracted significant attention [26,30–32] in TBG. Besides the conventional acoustic phonons, the moiré lattice allows for gapless shear modes, often referred to as *phasons*. Phason modes have a rich history in the study of quasicrystals [33] and charge-density-wave materials [34]. In our case, they can be intuitively thought of as the relative displacements of the two layers of TBG, which shift the moiré pattern and are thus gapless. However, a proper description [26,30] requires taking into account lattice relaxation, and the phasons then

correspond to the sliding of domain walls. Figure 1 illustrates that TTG allows for three types of long-wavelength phonon modes: on top of the regular acoustic phonons, where all three layers move in phase, there is another mirror-even set of modes, where the middle layer moves against the outer two layers. It is shown to be gapless and (modulo rescaling of parameters) exactly equivalent to the phasons of TBG. We further show that TTG also allows for mirror-odd shear modes, which have no analog in TBG and are found to be gapped; the existence of a gap is intuitively understood by noting that a mirror-odd displacement of the layers does not just correspond to a translation or rotation of the moiré pattern but rather to a nontrivial distortion of the superlattice.

In this work we not only investigate the twist-angle evolution of the phonon properties—which bear important consequences for the interpretation of experiments [12,13]— but also the impact of reduced electronic symmetries on the phonon spectrum. This includes both the effects of an applied displacement field or stacking shifts, which break the
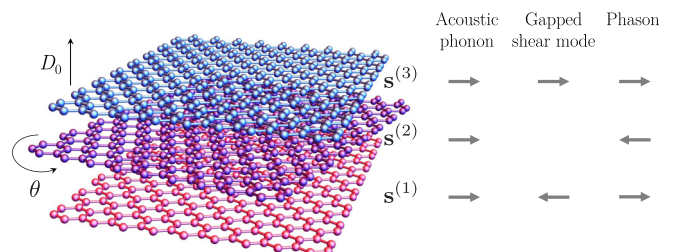

FIG. 1. Illustration of TTG in a perpendicular displacement field D_0 and its low-energy phonon modes.

mirror symmetry, leading to an admixture of the gapless and gapped shear modes, and the consequences of spontaneous electronic symmetry breaking. Theoretical [18–21] and experimental [6–13] studies of TTG indicate a variety of symmetry-broken electronic phases and studying their influence on the phonons is therefore crucial. We show how different electronic orders can induce finite angular momentum in the phonon branches.

Formalism. To begin, we first focus on the mirror-symmetric limit of TTG (i.e., in the absence of a displacement field) with no symmetry breaking in the electronic sector. The total free energy is a sum of two pieces $F = F_{el} + F_{ad}$, where F_{el} describes in-plane elastic distortions of the graphene layers and F_{ad} accounts for the interlayer adhesion energy. Labeling the layers from bottom to top by $l = 1, 2, 3$, and their corresponding in-plane [35] displacements by the two-component fields $\mathbf{s}^{(l)}$, the first term can be written as [36]

$$F_{el} = \sum_{l=1}^{3} \int dr \left[\frac{\lambda}{2} (\nabla \cdot \mathbf{s}^{(l)})^2 + \frac{\mu}{4} \left(\partial_i s_j^{(l)} + \partial_j s_i^{(l)} \right)^2 \right],$$

where $\lambda \simeq 3.25$ eV/Å^2 and $\mu \simeq 9.57$ eV/Å^2 are the Lamé coefficients of graphene [37,38]. We briefly discuss the out-of-plane field component in Sec. I C of the Supplemental Material (SM) [35]. The elastic theory is more naturally expressed in terms of the *relative* displacements, $\mathbf{u} \equiv \mathbf{s}^{(3)} - \mathbf{s}^{(1)}$ and $\mathbf{v} \equiv \mathbf{s}^{(3)} + \mathbf{s}^{(1)} - 2\mathbf{s}^{(2)}$, which are odd and even under mirror reflections, respectively, and the total displacement, $\mathbf{w} \equiv \mathbf{s}^{(1)} + \mathbf{s}^{(2)} + \mathbf{s}^{(3)}$ (cf. Fig. 1). While changes in $\mathbf{u}$ and $\mathbf{v}$ correspond to shear modes, the mode $\mathbf{w}$ represents an in-phase displacement of all three graphene sheets. The adhesion energy F_{ad} is a functional of the relative displacement fields only, i.e., $F_{ad} = \int dr \, \mathcal{V}_{ad}[\mathbf{r}, \mathbf{u}(\mathbf{r}), \mathbf{v}(\mathbf{r})]$, where $\mathcal{V}_{ad}$ represents the adhesion potential gluing the layers together; we expect $\mathcal{V}_{ad}$ to be well described as the sum of pairwise interlayer interactions between nearest-neighboring layers. Restricting its Fourier expansion to the smallest nonzero reciprocal lattice vectors $\mathbf{G}_\nu$, rotational symmetry implies that [35]

$$\mathcal{V}_{ad} = \sum_{l=1,3} V_l \sum_{\nu=1}^{3} \cos \left[\frac{\mathbf{b}_\nu}{2} \cdot (\mathbf{v} + p_l \mathbf{u}) - \mathbf{G}_\nu \cdot \mathbf{r} \right], \quad (1)$$

with $p_1 = -1$, $p_3 = +1$, where $\mathbf{b}_\nu$ are the reciprocal lattice vectors of a single graphene sheet; mirror symmetry implies $V_1 = V_3 \equiv V$. Putting F_{el} and F_{ad} together and solving the coupled Euler-Lagrange equations of motion for harmonic oscillations about the self-consistently determined equilibrium configurations $\{\mathbf{u}^{(0)}(\mathbf{r}), \mathbf{v}^{(0)}(\mathbf{r})\}$, we obtain the spectrum of lattice vibrations.

Mirror-symmetric limit. The relaxation of the moiré superlattice due to the interlayer couplings is captured by the displacement textures $\{\mathbf{u}^{(0)}, \mathbf{v}^{(0)}\}$. We see that this atomic reconstruction leads to a nontrivial $\mathbf{v}^{(0)} \neq 0$ [Fig. 2(b)], which illustrates that the lattice reorganizes itself to maximize (minimize) the regions of energetically (un)favorable AB/BA (AA) stackings in each bilayer. We find that this relaxation is equivalent to that of TBG, apart from a rescaling of parameters [35]. Furthermore, we obtain that $\mathbf{u}^{(0)}(\mathbf{r})$ is identically zero $\forall \, \mathbf{r}$. While spontaneous breaking of mirror symmetry by the lattice is possible in principle, $\mathbf{u}^{(0)} \neq 0$ is not favorable energetically.
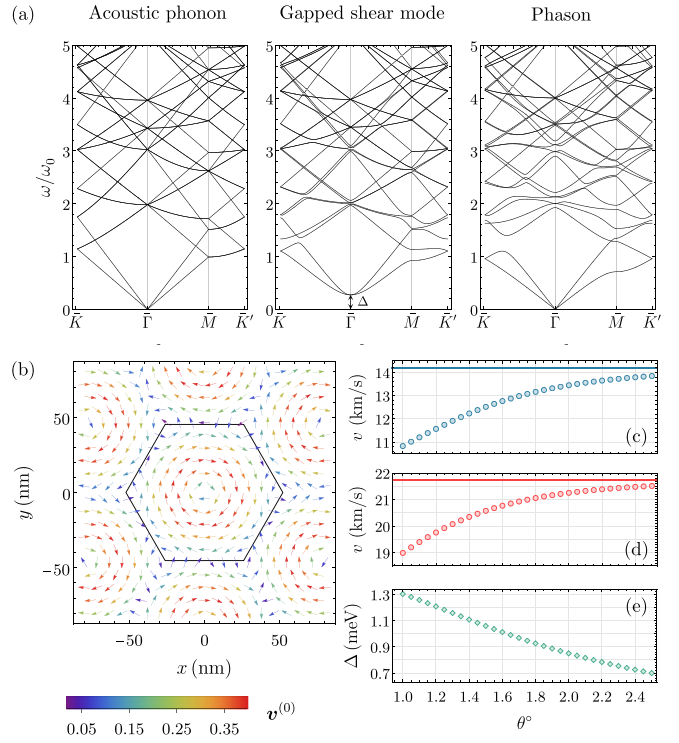

FIG. 2. (a) Phonon spectra of TTG in the mirror-symmetric limit at the magic angle $\theta = 1.56°$. (b) Lattice relaxation texture for $\mathbf{v}^{(0)}$; the AA (AB/BA) stacking regions at the center (corners) of the moiré unit cell—demarcated by the solid hexagon—shrink (expand) under such relaxation. (c, d) Phason velocities for the lowest two branches; the solid lines mark the transverse (v_{TA}, blue) and longitudinal (v_{LA}, red) acoustic phonon velocities. (e) Gap of the mirror-odd shear mode as a function of the twist angle.

This can be understood intuitively by noting that *simultaneous* maximization of local AB/BA stacking regions in the top and bottom bilayers via $\mathbf{v}^{(0)} \neq 0$ is most effective when the outer two layers are aligned, as seen in experiments [9,11].

The fully relaxed spectra of the three distinct classes of vibrational modes, arising from the displacements $\mathbf{u}$, $\mathbf{v}$, and $\mathbf{w}$, are arrayed in Fig. 2(a) in units of $\omega_0 = (2\pi/L_M)\sqrt{\lambda/\rho}$, where ρ is the mass density and L_M is the moiré lattice constant. Physically, the acoustic phonon modes, $\mathbf{w}(\mathbf{q})$, represent the in-phase vibrations of all three layers. On the other hand, the gapless *phason* modes, $\mathbf{v}(\mathbf{q})$, correspond to the sliding motion of the domain walls. As shown in Sec. I B of the SM [35], the phason mode for TTG is equivalent to that of TBG modulo rescaling of the adhesion potential $V \rightarrow 2V/3$. The phasons can be thought of as acoustic modes of the emergent moiré superlattice, and the soft nature of this lattice can be seen from the velocities in Figs. 2(c) and 2(d). Unlike the acoustic mode velocities, which, within the harmonic approximation, are just constants given by $v_{LA} = \sqrt{(\lambda + 2\mu)/\rho}$ and $v_{TA} = \sqrt{\mu/\rho}$, for longitudinal and transverse phonons, respectively, we see that the velocities of the low-frequency phason modes are extremely sensitive to twisting and can thus be used as an indirect probe to infer the twist angle. The existence of these soft phason modes is also expected to modify (and imprint signatures in) various experimental observables, including the

low-temperature specific heat [39], thermal conductivity [40], and frictional properties such as superlubricity [41–44].

Finally, there also exists a gapped shear mode, $\boldsymbol{u}(\boldsymbol{q})$, which is unique to TTG. This mode corresponds to a distortion of the moiré lattice and is thus massive, but the C_3 symmetry guarantees that the lowest two branches (the two polarizations) have the same mass. In Fig. 2(e) we see that the gap Δ decreases monotonically with increasing twist angles, and this behavior of the gap can be understood from the expression

$$\Delta^2 = \frac{3V}{2\rho}|\boldsymbol{b}|^2\alpha; \quad \alpha = \langle -\cos(\boldsymbol{b}_\nu \boldsymbol{v}^{(0)}/2 - \boldsymbol{G}_\nu \boldsymbol{r})\rangle_\Omega, \quad (2)$$

obtained from perturbation theory (see Eq. (S32) [35]). Here, $|\boldsymbol{b}| \equiv |\boldsymbol{b}_\nu|$, and $\langle \dots \rangle_\Omega$ denotes the spatial average over the system. Without any relaxation, i.e., $\boldsymbol{v}_0(\boldsymbol{r}) = 0$, we have $\alpha = 0$, while relaxation will result in $\alpha > 0$ to optimize the adhesion potential. This is also expected since, in the absence of relaxation, the top and bottom layers can be moved independently without any energetic cost in our elastic theory. Therefore the gap of the mirror-odd shear mode—a *thermodynamically observable* quantity—is directly proportional to the dimensionless measure α of lattice relaxation. Furthermore, we now also immediately understand that, for smaller twist angles, the impact of the relaxation will be stronger such that α, and hence, Δ, increases, in accordance with Fig. 2(e). Given that the gap varies from 10.5 to 5.6 cm^{-1} over this range of θ, the mirror-odd shear modes can be directly probed by Brillouin-Mandelstam spectroscopy [45,46].

Mirror-symmetry breaking. One particularly interesting aspect of TTG is that an electric displacement field D_0 can be applied perpendicular to the graphene layers (see Fig. 1), which breaks the mirror symmetry. D_0 is known to strongly affect the electronic degrees of freedom, as seen in experiments [6–13], and thus is expected to also modify the phononic properties. In our elastic theory, we model this phenomenologically by allowing for the adhesion potential strength to differ between the bottom and top bilayers, taking $V_{1,3} = V \mp \gamma D_0$ in Eq. (1).

The broken mirror symmetry has two crucial consequences. Firstly, while $\boldsymbol{v}^{(0)}$ continues to resemble the previously found profile in Fig. 2(b), lattice relaxation now also occurs in the mirror-odd sector, i.e., $\boldsymbol{u}^{(0)} \neq 0$. This can be seen in Figs. 3(a) and 3(b), where we plot the texture $\boldsymbol{u}^{(0)}(\boldsymbol{r})$, which closely follows that of $\boldsymbol{v}^{(0)}$, and how its strength evolves approximately linearly with γD_0. Specifically, we see that $\boldsymbol{u}^{(0)} \to \boldsymbol{v}^{(0)}/3$ as the extreme limit $\gamma D_0/V = 1$ is approached; this corresponds to the absence of relaxation in the top layer, which becomes completely decoupled in this case. While slightly unphysical, this limit helps us understand qualitatively the behavior of the second key modification—the change of the shear mode spectra. As can be seen in Fig. 3(c), the gapless phason mode at $D_0 = 0$ stays gapless for finite D_0 while the gap of the originally mirror-odd mode decreases. This is because the spectrum must approach that of the acoustic phonon of a single graphene layer and the phason of TBG (with doubled adhesion potential) in the above-mentioned limit of $\gamma D_0/V = 1$.

Another route to breaking mirror symmetry is via lateral stacking shifts [47], which naturally arise in experimental samples. For concreteness, let us consider a case in which
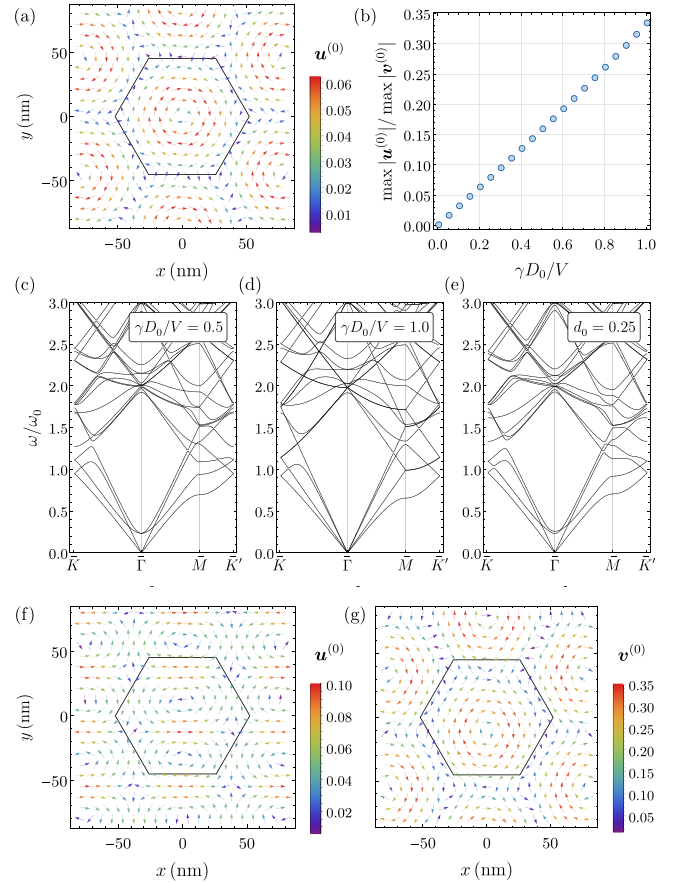

FIG. 3. (a) Mirror-odd lattice relaxation $\boldsymbol{u}^{(0)}$, and (b) its strength relative to the mirror-even $\boldsymbol{v}^{(0)}$ for $\theta = 1.56°$ TTG in the presence of a displacement field. (c, d) Spectra of shear modes as the field is varied. (e) The phonon spectrum for the shear modes when the mirror-symmetry breaking is induced by a lateral stacking shift of magnitude $d_0 = 0.25$; for clarity, we omit the acoustic phonons in (c–e). (f, g) The corresponding relaxation textures in this case.

the topmost layer is displaced from the original "A-twist-A" stacking by a vector $\boldsymbol{d} = d_0 \boldsymbol{a}/2$; here, $\boldsymbol{a}$ is chosen such that $d_0 = 1$ corresponds to "A-twist-B" stacking, which we find to be structurally unstable, as signaled by imaginary phonon frequencies. Interestingly, however, for $d_0 \lesssim 0.5$ we discover *metastable* configurations that are fundamentally distinct from our previous ones. This is most clearly seen from the lattice relaxation textures in Figs. 3(f) and 3(g): since $\boldsymbol{u}^{(0)}$ measures the static shift between the outer layers, the fact that it is a nonconstant vector (i.e., $\boldsymbol{u}^{(0)} \neq -\boldsymbol{d} \ \forall \ \boldsymbol{r}$) implies that the system does not just relax back to the earlier mirror-symmetric configuration but instead finds a different local minimum, oscillations about which yield the phonon spectrum in Fig. 3(e). The broken threefold rotational symmetry now lifts the prior degeneracy of the mirror-odd shear modes at the Γ point.

Spontaneous electronic symmetry breaking. Besides explicit symmetry breaking via external fields, TTG also exhibits a variety of electronic phases with spontaneously broken symmetry, as indicated by experiments [6–13]; some of these states coexist with superconductivity [6,7,10,13] and appear in the same regime of the phase diagram as the
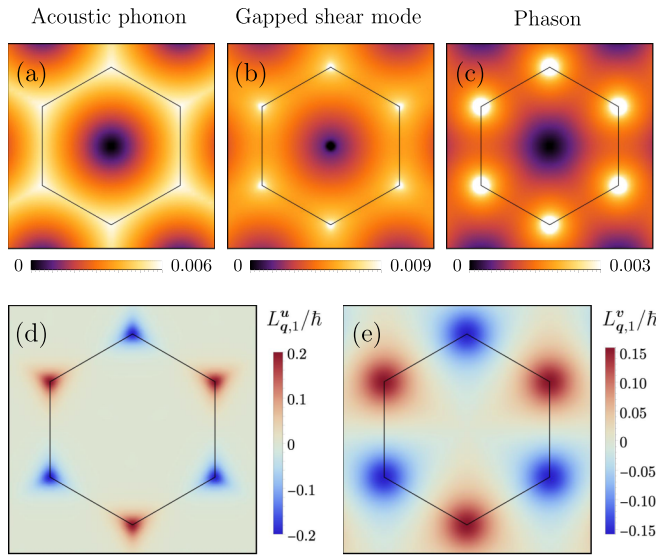
Acoustic phonon

Gapped shear mode

Phason

FIG. 4. Angular momentum of the lowest band of the (a) acoustic phonon, (b) gapped shear, and (c) phason modes in the presence of broken time-reversal symmetry at $\theta = 1.56°$, using a phenomenological value of $\eta/\sqrt{\rho} = 1$ (eV)$^{1/2}$ (see Fig. S4 [35] for the variation with η). The lower panel shows the angular momentum for the lowest band of the (d) gapped shear mode, and (e) phason when C_{2z} is broken for a value of $\phi = \pi/6$ (cf. Fig. S5 [35] for variation in ϕ). In this case, the angular momentum of the acoustic phonon is identically 0.

linear-in-T resistivity. As such, it is important to analyze the consequences of these electronic orders for the phonons. The combination $C_{2z}\Theta$ of time-reversal (Θ) and twofold-rotation symmetry (C_{2z}) is not only relevant to the stability of the electronic Dirac cones of the system but also for the phonon modes: the phononic angular momentum [48], $L_q^z = \int d\mathbf{r} \sum_{l=1}^{3} (\delta\mathbf{s}_q^{(l)} \times \delta\dot{\mathbf{s}}_q^{(l)})_z$, is constrained by Θ (C_{2z}) to obey $L_q^z = -L_{-q}^z$ ($L_q^z = L_{-q}^z$) and thus vanishes if $C_{2z}\Theta$ is a symmetry [49]. Recent theory [18] finds the emergence of sublattice-polarized phases at finite D_0, which break $C_{2z}\Theta$, gapping out all Dirac cones, in consistency with the more resistive behavior seen experimentally [6,7] in this regime. Whether this proceeds via breaking of C_{2z} or Θ depends on details of the exact interactions present and can be thought of as the spontaneous emergence of loop currents on the moiré scale with opposite or same chirality in the two valleys, respectively.

To begin with the latter, broken time-reversal symmetry induces a Hall viscosity term in the elastic theory [50,51], which, owing to C_{6z} rotation symmetry, can be parameterized (Sec. SIII B [35]) by a single real number, η, as $F_\eta = \eta \int d\mathbf{r} \sum_l ([\partial_j^2 \delta\mathbf{s}^{(l)}] \times \delta\dot{\mathbf{s}}^{(l)})_z$. Here η has to scale as $\eta \sim g^2 M$ for small electron-phonon coupling strength g and magnitude M of the sublattice polarization [52]. As shown in Figs. 4(a)–4(c), this induces a finite angular momentum in all low-energy modes, the overall scale of which increases with η [35]. Most importantly, by virtue of resulting from broken Θ rather than C_{2z} symmetry, the integral of L_q^z over the Brillouin zone of a given band does not vanish, which crucially differs from previous discussions of angular momentum bands in

moiré systems [53,54]. Interestingly, the contributions from the different modes have the same sign, as opposed to acoustic and optical phonons in regular crystals [48]. Consequently, the phononic system exhibits a finite ground-state angular momentum, which has to decay at sufficiently large temperature due to the Bohr–van Leeuwen theorem. Fingerprints of the angular momenta in the phononic bands could potentially even be probed experimentally via the Einstein–de Haas effect [48] or the phonon thermal Hall effect [55], which has attracted much attention recently in the context of cuprate superconductors [56] and Kitaev materials [57]. For completeness, we also studied [35] sublattice polarization which breaks C_{2z} instead of Θ; practically, this corresponds to adding a phase ϕ to each cosine of $\mathcal{V}_{ad}$ in Eq. (1). In this case, L_q^z is odd in q, as clearly seen in Figs. 4(d) and 4(e), and the net angular momentum vanishes at any temperature.

Discussion. Making the natural [10] assumption that electron-phonon coupling is an important driving force of superconductivity in TBG and TTG, our results provide a natural explanation for why both systems show superconductivity with comparable T_c. As we have shown, the phason modes are equivalent in the two systems, modulo an $\mathcal{O}(1)$ rescaling of parameters, and we expect the additional mirror-odd mode to only provide a subleading enhancement of T_c for vanishing D_0, since it couples the flat (TBG-like) bands to the highly dispersive (graphenelike) bands of TTG. When turning on a finite D_0, the two sectors mix and we expect the gapped shear mode to become more relevant; this might play an important role in the observed enhancement [6] of superconductivity for small D_0. In this picture our results are also consistent with recent experiments, where the transition temperature was found to be approximately the same at the magic angle ($\theta \simeq 1.5°$) and in the "small-twist-angle regime" ($\theta \simeq 1.3°$) [58], since we find that the phonon properties change by only a small amount in this range of θ, see Figs. 2(c)–2(e).

If electron-phonon coupling is also responsible for the linear-in-T resistivity, $\varrho \propto T$, which is considered to be a plausible scenario [23–26], the observed suppression [12] of it around $\theta = 1.3°$ will have to be due to at least one of the following reasons: (i) the temperature scale below which phonons do not give rise to a linear-in-T contribution increases significantly. This temperature scale is an $\mathcal{O}(1)$ fraction [59] of the Bloch-Grüneisen-like temperature scale $T_{BG} = \omega(\mathbf{k}^*)$, where $\mathbf{k}^*$ is the characteristic momentum transfer required to change the direction of the electronic group velocity significantly. Choosing $\mathbf{k}^*$ to be half the vector connecting the Γ and K point as an example, we find $T_{BG} \simeq 25$ K and 30 K for the mirror-even and mirror-odd modes at $\theta = 1.5°$. These scales even decrease further, to 18 K and 24 K, respectively, when reducing the angle to $\theta = 1.3°$. So we are left with possibility (ii) that the magnitude of the phonon-induced contribution to ϱ decreases rapidly with θ. Focusing on the gapless phason mode, the slope $d\varrho/dT$ is proportional to [24,26] $|g|^2/(v_F^2 \rho_m v_{ph}^2)$, where g is the electron-phonon coupling matrix element, v_F (v_{ph}) the Fermi (phonon) velocity, and $\rho_m \propto \sin(\theta/2)$ the soliton-network mass density [26]. From our phonon spectra, we find $\rho_m v_{ph}^2$ decreases by about 20% from $\theta = 1.5°$ to $1.3°$, corresponding to an increased contribution to ϱ. Furthermore, the approximately identical phonon spectra at these two angles imply that the resulting

superconducting T_c should be primarily determined by $|g|^2/v_F$, since the density of states at a fixed filling fraction scales as $1/v_F$. Experimentally, T_c is seen [12] to be about the same for the two angles, so the only way to explain the absence of linear-in-T behavior at small θ is if v_F increases significantly from $\theta = 1.5°$ to $1.3°$; this, however, is not plausible either, as the measured [12] bandwidth is even smaller in the small-twist-angle regime. Consequently, the recent data of Ref. [12] is not consistent with a picture based on phonons alone and points towards another origin. This is not only in accordance with a very recent low-temperature study on TBG [60] but is also reminiscent of transport behavior in the "strange metal" phase of the cuprate superconductors [61].

[1] A. H. MacDonald, Physics **12**, 12 (2019).
[2] E. Y. Andrei and A. H. MacDonald, Nat. Mater. **19**, 1265 (2020).
[3] D. M. Kennes, M. Claassen, L. Xian, A. Georges, A. J. Millis, J. Hone, C. R. Dean, D. N. Basov, A. N. Pasupathy, and A. Rubio, Nat. Phys. **17**, 155 (2021).
[4] L. Balents, C. R. Dean, D. K. Efetov, and A. F. Young, Nat. Phys. **16**, 725 (2020).
[5] M. S. Scheurer, Nature (London) **572**, 40 (2019).
[6] J. M. Park, Y. Cao, K. Watanabe, T. Taniguchi, and P. Jarillo-Herrero, Nature (London) **590**, 249 (2021).
[7] Z. Hao, A. M. Zimmerman, P. Ledwith, E. Khalaf, D. H. Najafabadi, K. Watanabe, T. Taniguchi, A. Vishwanath, and P. Kim, Science **371**, 1133 (2021).
[8] Y. Cao, J. M. Park, K. Watanabe, T. Taniguchi, and P. Jarillo-Herrero, arXiv:2103.12083.
[9] H. Kim, Y. Choi, C. Lewandowski, A. Thomson, Y. Zhang, R. Polski, K. Watanabe, T. Taniguchi, J. Alicea, and S. Nadj-Perge, arXiv:2109.12127.
[10] X. Liu, N. J. Zhang, K. Watanabe, T. Taniguchi, and J. I. A. Li, arXiv:2108.03338.
[11] S. Turkel, J. Swann, Z. Zhu, M. Christos, K. Watanabe, T. Taniguchi, S. Sachdev, M. S. Scheurer, E. Kaxiras, C. R. Dean, and A. N. Pasupathy, Science **376**, 193 (2022).
[12] P. Siriviboon, J.-X. Lin, X. Liu, H. D. Scammell, S. Liu, D. Rhodes, K. Watanabe, T. Taniguchi, J. Hone, M. S. Scheurer, and J. I. A. Li, arXiv:2112.07127.
[13] P. Siriviboon, J.-X. Lin, X. Liu, H. D. Scammell, S. Liu, D. Rhodes, K. Watanabe, T. Taniguchi, J. Hone, M. S. Scheurer, and J. I. A. Li, arXiv:2112.07127 [cond-mat.mes-hall].
[14] W. Qin and A. H. MacDonald, Phys. Rev. Lett. **127**, 097001 (2021).
[15] A. Fischer, Z. A. H. Goodwin, A. A. Mostofi, J. Lischner, D. M. Kennes, and L. Klebl, npj Quantum Mater. **7**, 5 (2022).
[16] Y.-Z. Chou, F. Wu, J. D. Sau, and S. Das Sarma, Phys. Rev. Lett. **127**, 217001 (2021).
[17] E. Lake and T. Senthil, Phys. Rev. B **104**, 174505 (2021).
[18] M. Christos, S. Sachdev, and M. S. Scheurer, Phys. Rev. X **12**, 021018 (2022).
[19] F. Xie, N. Regnault, D. Călugăru, B. A. Bernevig, and B. Lian, Phys. Rev. B **104**, 115167 (2021).
[20] H. D. Scammell, J. I. A. Li, and M. S. Scheurer, 2D Mater. **9**, 025027 (2022).
[21] P. J. Ledwith, E. Khalaf, Z. Zhu, S. Carr, E. Kaxiras, and A. Vishwanath, arXiv:2111.11060.
[22] Y. Cao, D. Chowdhury, D. Rodan-Legrain, O. Rubies-Bigorda, K. Watanabe, T. Taniguchi, T. Senthil, and P. Jarillo-Herrero, Phys. Rev. Lett. **124**, 076801 (2020).
[23] H. Polshyn, M. Yankowitz, S. Chen, Y. Zhang, K. Watanabe, T. Taniguchi, C. R. Dean, and A. F. Young, Nat. Phys. **15**, 1011 (2019).
[24] F. Wu, E. Hwang, and S. Das Sarma, Phys. Rev. B **99**, 165112 (2019).
[25] I. Yudhistira, N. Chakraborty, G. Sharma, D. Y. H. Ho, E. Laksono, O. P. Sushkov, G. Vignale, and S. Adam, Phys. Rev. B **99**, 140302(R) (2019).
[26] H. Ochoa, Phys. Rev. B **100**, 155426 (2019).
[27] P. Stepanov, I. Das, X. Lu, A. Fahimniya, K. Watanabe, T. Taniguchi, F. H. L. Koppens, J. Lischner, L. Levitov, and D. K. Efetov, Nature (London) **583**, 375 (2020).
[28] X. Liu, Z. Wang, K. Watanabe, T. Taniguchi, O. Vafek, and J. I. A. Li, Science **371**, 1261 (2021).
[29] Y. Saito, J. Ge, K. Watanabe, T. Taniguchi, and A. F. Young, Nat. Phys. **16**, 926 (2020).
[30] M. Koshino and Y.-W. Son, Phys. Rev. B **100**, 075416 (2019).
[31] J. Gaa, G. Palle, R. M. Fernandes, and J. Schmalian, Phys. Rev. B **104**, 064109 (2021).
[32] H. Ochoa and R. M. Fernandes, Phys. Rev. Lett. **128**, 065901 (2022).
[33] D. Levine, T. C. Lubensky, S. Ostlund, S. Ramaswamy, P. J. Steinhardt, and J. Toner, Phys. Rev. Lett. **54**, 1520 (1985).
[34] S. Sugai, Y. Takayanagi, and N. Hayamizu, Phys. Rev. Lett. **96**, 137003 (2006).
[35] See Supplemental Material, which includes Refs. [63–72], at http://link.aps.org/supplemental/10.1103/PhysRevB.106.L201403 for further details on the elastic theory of moiré phonons, the phonon spectra, and the impact of electronic symmetry breaking as it relates to the phonon angular momentum.
[36] H. Suzuura and T. Ando, Phys. Rev. B **65**, 235412 (2002).
[37] K. V. Zakharchenko, M. I. Katsnelson, and A. Fasolino, Phys. Rev. Lett. **102**, 046808 (2009).
[38] J. Jung, A. M. DaSilva, A. H. MacDonald, and S. Adam, Nat. Commun. **6**, 6308 (2015).

[39] D. L. Nika, A. I. Cocemasov, and A. A. Balandin, Appl. Phys. Lett. **105**, 031904 (2014).

[40] H. Li, H. Ying, X. Chen, D. L. Nika, A. I. Cocemasov, W. Cai, A. A. Balandin, and S. Chen, Nanoscale **6**, 13402 (2014).

[41] I. Maity, M. H. Naik, P. K. Maiti, H. R. Krishnamurthy, and M. Jain, Phys. Rev. Res. **2**, 013335 (2020).

[42] E. Koren and U. Duerig, Phys. Rev. B **93**, 201404(R) (2016).

[43] E. Koren and U. Duerig, Phys. Rev. B **94**, 045401 (2016).

[44] W. Wang, J. Shen, and Q.-C. He, Phys. Rev. B **99**, 054103 (2019).

[45] S. Speziale, H. Marquardt, and T. S. Duffy, Rev. Mineral. Geochem. **78**, 543 (2014).

[46] F. Kargar, B. Debnath, J.-P. Kakko, A. Säynätjoki, H. Lipsanen, D. L. Nika, R. K. Lake, and A. A. Balandin, Nat. Commun. **7**, 13400 (2016).

[47] C. Lei, L. Linhart, W. Qin, F. Libisch, and A. H. MacDonald, Phys. Rev. B **104**, 035139 (2021).

[48] L. Zhang and Q. Niu, Phys. Rev. Lett. **112**, 085503 (2014).

[49] More generally, it vanishes if there is a valley-U(1) or spin rotation that, when combined with $C_{2z}\Theta$, is a symmetry.

[50] J. E. Avron, R. Seiler, and P. G. Zograf, Phys. Rev. Lett. **75**, 697 (1995).

[51] J. E. Avron, J. Stat. Phys. **92**, 543 (1998).

[52] Y. Zhang, Y. Teng, R. Samajdar, S. Sachdev, and M. S. Scheurer, Phys. Rev. B **104**, 035103 (2021).

[53] N. Suri, C. Wang, Y. Zhang, and D. Xiao, Nano Lett. **21**, 10026 (2021).

[54] I. Maity, A. A. Mostofi, and J. Lischner, Phys. Rev. B **105**, L041408 (2022).

[55] T. Qin, Q. Niu, and J. Shi, Phys. Rev. Lett. **107**, 236601 (2011).

[56] G. Grissonnanche, S. Thériault, A. Gourgout, M.-E. Boulanger, E. Lefrançois, A. Ataei, F. Laliberté, M. Dion, J.-S. Zhou, S. Pyon, T. Takayama, H. Takagi, N. Doiron-Leyraud, and L. Taillefer, Nat. Phys. **16**, 1108 (2020).

[57] E. Lefrançois, G. Grissonnanche, J. Baglo, P. Lampen-Kelley, J.-Q. Yan, C. Balz, D. Mandrus, S. E. Nagler, S. Kim, Y.-J. Kim, N. Doiron-Leyraud, and L. Taillefer, Phys. Rev. X **12**, 021025 (2022).

[58] J.-X. Lin, P. Siriviboon, H. D. Scammell, S. Liu, D. Rhodes, K. Watanabe, T. Taniguchi, J. Hone, M. S. Scheurer, and J. I. A. Li, Nat. Phys. **18**, 1221 (2022).

[59] E. H. Hwang and S. Das Sarma, Phys. Rev. B **77**, 115449 (2008).

[60] A. Jaoui, I. Das, G. Di Battista, J. Díez-Mérida, X. Lu, K. Watanabe, T. Taniguchi, H. Ishizuka, L. Levitov, and D. K. Efetov, Nat. Phys. **18**, 633 (2022).

[61] S. Sachdev and D. Chowdhury, Prog. Theor. Exp. Phys. **2016**, 12C102 (2016).

[62] Q. Gao and E. Khalaf, Phys. Rev. B **106**, 075420 (2022).

[63] S. Dai, Y. Xiang, and D. J. Srolovitz, Nano Lett. **16**, 5923 (2016).

[64] S. Carr, C. Li, Z. Zhu, E. Kaxiras, S. Sachdev, and A. Kruchkov, Nano Lett. **20**, 3030 (2020).

[65] I. V. Lebedeva, A. A. Knizhnik, A. M. Popov, Y. E. Lozovik, and B. V. Potapkin, Phys. Chem. Chem. Phys. **13**, 5687 (2011).

[66] A. M. Popov, I. V. Lebedeva, A. A. Knizhnik, Y. E. Lozovik, and B. V. Potapkin, Phys. Rev. B **84**, 045404 (2011).

[67] A. I. Cocemasov, D. L. Nika, and A. A. Balandin, Phys. Rev. B **88**, 035428 (2013).

[68] X. Gong and E. J. Mele, Phys. Rev. B **89**, 121415 (2014).

[69] S. Zhou, J. Han, S. Dai, J. Sun, and D. J. Srolovitz, Phys. Rev. B **92**, 155438 (2015).

[70] N. N. T. Nam and M. Koshino, Phys. Rev. B **96**, 075311 (2017).

[71] S. Carr, D. Massatt, S. B. Torrisi, P. Cazeaux, M. Luskin, and E. Kaxiras, Phys. Rev. B **98**, 224102 (2018).

[72] L. Zhang and Q. Niu, Phys. Rev. Lett. **115**, 115502 (2015).